

The influence of scattered photons on the accurate determination of microcalcification thickness in digital mammography

Varlen Grabski and Maria-Ester Brandan

Instituto de Fisica, UNAM, A. P. 20-364, 01000, D.F., Mexico

E-mail: grabski@fisica.unam.mx, varlen.grabski@cern.ch

Abstract. Our interest has been to study the effect that scattered radiation has on contrast, signal-to-noise ratio and thickness reconstruction in digital mammographies. Using the GEANT code we have performed Monte-Carlo simulations of 25 kVp Mo/Mo photons, through a breast phantom which contains a 0.2-1.0 mm thick microcalcifications incident on a $20 \times 106 \text{ mm}^2$ pixelized detector. The data have been analyzed assuming 6 different shapes of the incident beam: a $0.2 \times 0.2 \text{ mm}^2$ "narrow" beam, 4 different 20 mm long scanning beams of various widths, and a $20 \times 100 \text{ mm}^2$ beam with no scatter reduction mechanisms (NSR). Since the image of a point depends on scattered photons which passed up to 2 cm away from the object (for 4 cm thick phantom), we identify the background definition as a main source of systematic uncertainty in the image quality analysis. We propose the use of two dimensional functions (a polynomial for the background and Gaussians for the signal) for total photon transmission description. Our main results indicate the possible calcification thickness reconstruction with an accuracy of the order of 6% using 3 mm wide scanning beam. Signal-to-noise ratio with the 3 mm wide beam gets improved by 20% with respect to NSR , a figure similar to that obtained with the narrow beam. Thickness reconstruction is shown to be an alternative to signal-to-noise ratio for microcalcification detection.

PACS numbers: 07.05.Pj, 42.30.Va, 87.57.-s

Submitted to: *PBM*

1. Introduction

One of the main limitations of image reconstruction in mammography, independent of external geometry and total breast thickness, is the influence of scattered photons. The main parameter used to describe scattered photon contributions is scatter-to primary radiation ratio (SPR), which has been measured[1] and calculated [2], and is $\sim 0.5 - 0.6$ for typical voltages and breast phantom dimensions. The presence at the image receptor of photons which have been scattered by the breast tissue components results in a severe loss of contrast. The contrast reduction is estimated to be about ~ 0.6 for the above SPR, and the range of values encountered in mammography indicates that the contrast can be improved by factors of $\sim 1.4 - 2.5$ if scattered radiation is eliminated from the image [3]. The most popular solution for the problem has been the use of antiscatter grids in mammography units [4]. These improve the contrast by typical factors of $\sim 1.2 - 1.4$ but also reduce the primary intensity, resulting in a patient dose increase of approximately 2 for typical mammographic conditions [4] in order to reach the necessary photon fluence for a good quality image. Lately, the use of scanning narrow beams [5, 6], a direct way to reduce the volume of the irradiated scattering medium, has found its way into commercial mammographic systems.

Mammographic systems using digital detectors offer distinct advantages with respect to the conventional screen/film image recorder due to their much wider dynamical range of useful exposures. Since the response of the detector is linear over some 4 orders of magnitude in exposure, there is no need to increase exposure if scattering reduction methods are used, and the signal detection limit is dominated by the signal-to-noise ratio (*SNR*) [7]. Another parameter which can be used to evaluate the digital image quality is the linear size of the object along the photon direction, as evaluated from the image. This thickness can be determined by using the visual contrast (VC) [8] and the linear absorption coefficients. Clinically, the correct determination of this parameter, for instance, a microcalcification (μC) thickness, can be an indicator of the stage of development of this formation. Though we consider the thickness parameter to be of more evident and real character than the contrast, it is necessary to determine which of these two is more sensitive, both for the microcalcification detection and its study as well.

In this work we have performed Monte Carlo (M-C) simulations of the passing of photons through a breast phantom which contains a few μC of different thickness inside. The influence of the scattered photons on the contrast, *SNR* and thickness determination has been studied for a variety of incident beam definitions, using a scanning slit as the scatter reduction technique.

2. The model

At least two X-ray transmission measurements are necessary to recover each of the components of a simulated three-component breast (microcalcification, adipose and glandular tissue), if the total thickness is known[11]. This task can be considerably simplified under the assumption that one of the components has constant thickness; this will lead to a two-component model, for which one measurement is enough. The phantom proposed in this work assumes that microcalcifications are embedded in the glandular tissue, and that constant-thickness adipose tissue covers the outside of the breast. The geometry and the structure of the proposed breast phantom model is shown in Fig. 1. The phantom, with lateral dimensions $10 \times 10 \text{ cm}^2$, has

a total thickness of 4 cm. Two adipose layers cover the top and bottom sides with a total thickness of 1 cm, and 3 cm thick glandular tissue is located between the adipose layers. Five μC are located at the midplane of the glandular tissue layer. The microcalcifications are cylindrical in shape, 4 mm diameter, and have variable thicknesses between 0.2 and 1.0 mm. The selection of a 25 percent adipose component is done for the purpose of increasing the relative contribution of the noise[11]. The detailed chemical compositions of the phantom materials are presented in table 1. All estimates, and the M-C simulations, have been carried out with this simplified model of the breast.

In order to understand the difficulties to recover the μC dimensions from a radiological image, let us conduct some estimations for mono-energetic photons, neglecting the effects of scattering. In the absence of μC , the number of photons passing through the phantom ($N_{nc}(x, y)$) is defined through the total number of $N_0(x, y)$ primary photons as:

$$N_{nc}(x, y) = N_0(x, y) \exp(-\mu_a t_a(x, y) - \mu_g t_g(x, y)), \quad (1)$$

where μ_a and μ_g are the linear absorption coefficients, and t_a and t_g are the thickness of the adipose and glandular tissues, respectively. With the addition of μC , Eqn. (1) transforms into:

$$N_c(x, y) = N_0(x, y) \exp(-\mu_a t_a(x, y) - \mu_g t_g^c(x, y) - \mu_c t_c(x, y)), \quad (2)$$

where μ_c is the microcalcification linear attenuation coefficient, and $t_c(x, y)$ is its thickness. $N_c(x, y)$ is the number of the transmitted photons in the presence of calcifications. Within our simplified model, $t_g^c(x, y)$ will be defined as:

$$t_g^c(x, y) = t_g(x, y) - t_c(x, y). \quad (3)$$

Dividing Eqn. (1) into (2) and taking logarithms, we obtain the following for the μC thickness t_c :

$$t_c(x, y) = D_\mu^{-1} \log(N_{nc}(x, y)/N_c(x, y)), \quad (4)$$

where $D_\mu = \mu_c - \mu_g$. To be correct, linear attenuation coefficients such as those in the NIST data base, should be used only for the narrow-beam condition[13] since they do not include the effect of the scatter radiation. Thus, within this approximation, the μC thickness can be easily determined by one measurement in which the value of N_{nc} is determined from the region outside the microcalcification. However, in reality, the determination of N_{nc} is only approximate because the effects of scattering, geometry and the inner structure of the breast tissue can introduce several inaccuracies.

The contrast parameter, traditionally used in conventional mammography, is useless in digital mammography since the possibility of detecting the signal depends on the SNR [7], defined as:

$$SNR = (N_{nc} - N_c)/\sqrt{N_{nc} + N_c}. \quad (5)$$

The important question is the choice of the most appropriate parameter to use for the accomplishment of the image quality optimization.

Let us compare SNR and μC thickness to determine which one is more sensitive for the detection of the μC . The ratio R , between the relative errors in the determination of each parameter, is:

$$R = (\sigma_{t_c}/t_c)/(\sigma_{SNR}/SNR) = \frac{1-m}{\sqrt{m} \cdot \log(1/m)}, \quad (6)$$

where σ_{t_c} and σ_{SNR} are the uncertainties in the determination of thickness and SNR , respectively, t_c and SNR are given by Eq 4 and 5, respectively, and $m = N_c/N_{nc}$. When $m \rightarrow 1$, which corresponds to a thin μC , relation (6) approaches 1, which indicates the equivalence of t_c and SNR parameters for the detection of the μC , and the relative uncertainties of both parameters have identical statistical behavior, $\sim 1/\sqrt{N_{nc}}$. On the other hand, in case of a given fluence, the statistics are proportional to the object surface so the relative statistical uncertainty in the object image will depend on $1/r$, where r is the object linear size. Consequently, the measurement of the μC thickness is not less sensitive than measuring the SNR or contrast in the detection of the μC and, at the same time, makes possible to restore the μC three dimensions.

Everything stated above is correct in the absence of scattering. After switching scattering on, the description becomes more complicated and conducting estimations is complex and dependent on the geometry and structure of the breast. This problem can be easily solved using a simulation of the photon transport through the phantom volume.

3. Monte-Carlo simulation

There are two different possibilities for M-C simulation of the photon transport process in the phantom. The results of M-C simulations based on the convolution method [2] (also known as “fast” M-C simulation), are sensitive to geometry and beam parameters. This is why it is necessary to estimate the possible systematic uncertainties of the method each time it is used when geometry, medium, beam size, etc are changed. The method that we use in this work (“full” simulation) is based on the individual transport of each photon. It is not as fast as convolution, but is more accurate when describing the concrete experimental conditions. The choice of the method depends on the task. In our opinion, the code GEANT[12] is a very good choice for this purpose. This powerful Monte Carlo program was built for the transport of elementary particles through matter, and includes all processes of low energy photon interactions which are relevant for the transport of typical mammography X-rays. This program, which has been tested to be appropriate for the high-energy region, it is now more and more frequently used in medical physics[14]. GEANT4 is flexible enough for the required additional programming in C++, and is user-friendly. To reconstruct the thicknesses from the photon intensities at the image detector plane we will use mass attenuation coefficients from the NIST data base [10]. The mass attenuation coefficients for tissue components and calcium carbonate are calculated using percentages per weight according to [13] and NIST and shown in Table 1. Our estimates indicate that the agreement between these mass coefficients data and GEANT internal cross sections for the physical processes is not worse than 2 percent in the energy region below 25 keV. At this stage, this agreement is sufficient to study the influence of scattering on the accuracy of the thickness determination. To use

the code it is necessary to describe the photon beams incident on the phantom and the geometry and composition of the detector. The simulated experimental setup is shown in Fig. 2. Almost all significant characteristics of the digital mammography unit Senographe 2000D (GE Medical Systems) have been incorporated in this setup with the purpose to assume parameters of an existing system. No antiscatter grid is being used. For the photon beam, a typical X-ray spectrum for 25 kVp Mo/Mo target/filter combination has been used [15]. The angular distribution of X-rays on the phantom has been assumed uniform. Photons have been detected by pixelized $0.1 \times 0.1 \times 0.1 \text{ mm}^3$ CsI(Tl) scintillators covering a total area equal $20 \times 106 \text{ mm}^2$. The beam size on phantom was $20 \times 106 \text{ mm}^2$, equal to the detector size, with the purpose of decreasing the simulation time. The total number of primary photons incident on the $\sim 21 \text{ cm}^2$ phantom surface is $\sim 1.8 \times 10^9$, which corresponds to a normalized glandular dose $\sim 0.03 \text{ mGy}$ [16]. This dose is rather low compared with the usual values in mammography. The results of the simulation have been stored in binary files for the offline analysis, performed by a program, that uses the mathematical and graphic library ROOT[17].

4. Results and discussion

The simulated data were analyzed assuming 6 different shapes of the incident beam. All these beams have rectangular shapes on the phantom. The “ideal” beam is narrow with dimensions $0.2 \times 0.2 \text{ mm}^2$. For the other beams, one dimension is always equal to the width of the detector (20 mm) and the other is variable. We use the following nomenclature:

$0.2 \times 0.2 \text{ mm}^2$, “narrow” beam;
 $1 \times 20 \text{ mm}^2$, 1mm wide scanning beam ;
 $3 \times 20 \text{ mm}^2$, 3mm wide scanning beam;
 $5 \times 20 \text{ mm}^2$, 5mm wide scanning beam ;
 $10 \times 20 \text{ mm}^2$, 10mm wide scanning beam ;
 $20 \times 100 \text{ mm}^2$, “NSR”, non-scattering reduction.

Data scanning was done along the detector long axis and beam size was controlled by the collimator placed between the X-ray source and the phantom. For the simulation of the scanning beam, the analysis included only the data generated by photons incident within a collimator region. The NSR regime didn't use any scan.

In order to determine the characteristic size of the region of scattered photons, in Fig 3 we have plotted the distribution of scattered photons, point spread function (PSF), as a function of Dx (coordinate difference between the initial and the scattered photons position). The spot size defined as the PSF (root-mean-squared) is $\sim 1 \text{ cm}$. For our geometry the SPR is 0.39, which agrees with similar M-C [2] calculations for 4 cm thick phantoms and 25 kVp X-rays. The distribution in Fig. 3 shows that the image of each point depends on photons that pass up to 2 cm away from the point. This value depends on the geometry and will increase as a function of total phantom thickness. This result also indicates that, in order to determine the value of N_{nc} , it is necessary to define a distance more than 2 cm away from the μC . But, this distance is sufficiently large for the structure and geometry of the phantom to have changed. That's why we suggest a different procedure of background calculation.

The total signal $F(x, y)$ in the image (distribution of photons on the detector) can be expressed as the sum of the μC and the background signals, where the background

$P(x, y)$ is supposed to show smooth behavior and the μC signal $G(x, y)$ is described using a Gaussian function:

$$F(x, y) = P(x, y) + \Sigma G(x, y), \quad (7)$$

where $P(x, y)$ is a two-dimensional polynomial of order three and $G(x, y)$ is a two-dimensional Gaussian function for each target μC . The parameters of this function have been defined by fits on simulation $N_c(x, y)$ data. The number of parameters in $F(x, y)$ is 25 and the number of points ~ 8000 . The value of χ^2 per point is typically 1.5 - 2.5 which is not bad (taking into account the approximate description of the signal with Gaussian shapes). The description of the target images as having Gaussian shapes may not be the best, but it makes the task easier. After defining its parameters by fit, the function $P(x, y)$ has been used as the background instead of $N_{nc}(x, y)$ in the SNR , contrast and thickness definitions. A symmetric noise in the thickness, SNR and contrast definitions with respect to zero, indicates that the fit is appropriate.

The $F(x, y)$ for all the events (20x106 mm^2 X-ray beam) is plotted in Fig 4. The decreasing values of $F(x, y)$ near the edges of the detector can be explained as a geometrical and scattering effect. By using an extreme scatter reduction method (0.2x0.2 mm^2 X-ray beam), as shown in Fig. 5, it is possible to make the background behavior more flat ($\pm 1\%$ compared with a plane surface). To reduce the number of parameters, the standard deviations σ_x and σ_y for each Gaussian-shaped μC have been set equal ($\sigma_x = \sigma_y$). The calculated diameters for all μC are plotted in Fig 6. Error bars are parameter errors obtained during the fit. The overestimations of the transversal sizes (diameter) ($\sim 25\%$) can be explained as the consequence of a not-totally appropriate description of the signal by the Gaussian functions. The thickness dependence of the (calculated /original) μC diameter ratio in Fig. 6 can be explained as the increase of scattering as a function of the μC thickness.

The SNR is defined as:

$$SNR(x, y) = (P(x, y) - N_c(x, y)) / \sqrt{(\sigma_{P(x, y)})^2 + N_c(x, y)}, \quad (8)$$

where $\sigma_{P(x, y)}$ is the definition uncertainty of the $P(x, y)$, which should be smaller than $\sqrt{P(x, y)}$. In the calculations we have used the value $\sqrt{P(x, y)}$ for $\sigma_{P(x, y)}$.

The contrast C is defined as:

$$C(x, y) = (P(x, y) - N_c(x, y)) / P(x, y). \quad (9)$$

The thickness t_c is defined as:

$$t_c(x, y) = D_\mu^{-1} \log(P(x, y) / N_c(x, y)) \quad (10)$$

and, from the fits, t_f is defined as:

$$t_f(x, y) = D_\mu \log(P(x, y) / F(x, y)) \quad (11)$$

where $N_c(x, y)$ is the number of photons detected in the pixel detector, and D_μ is the difference between mean values of the linear attenuation coefficients for μC and

glandular tissue. The results for t_f are shown in Fig 7 as the ratio of the reconstructed (Gaussian maximum for each target) value from Eqn.(11) to the original thicknesses, for the “narrow” beam. For the other beams, we show their ratio with respect to the “narrow”. In order to get the correct thickness for the 200 μm calcifications it is necessary to make a correction due the peaked value of the Gaussian shape (suggested correction: a 0.73 factor on signal value ($P(x, y) - F(x, y)$) for the 200 μm and slowly increasing up to 0.80 for 1000 μm). As we have mentioned before, the Gaussian fit is not optimum for these cylindrical target shapes (diameter/thickness ratio is $\sim 4 - 20$) because the flat tops are noticeable in the image.

Results of the 3-dimensional reconstructed distributions of $t_c(x, y)$, $SNR(x, y)$ and $C(x, y)$ for our phantom are shown in Figs. 8 - 10. These distributions have been used to determine the mean values of the thickness, SNR and contrast of the targets. To reduce statistical errors we have calculated the mean values of the thickness only for the cases where they are greater than the original thickness minus 3 noise values. The central target is 200 μm thick and the collected statistics is enough to have a signal 10 standard deviations above the noise for the ‘narrow’ beam (see Fig 8). For the 200 μm thick μC , the signal to noise ratio is ~ 10 , (Fig 9) which agrees with our statement that thickness and SNR have similar sensitivities for μC detection. The bin size of the histograms is 0.5x0.5 mm^2 . The same level of statistical errors for the detector pixel size (0.1x0.1 mm^2) can be reached increasing the dose approximately 25 times that is 0.75 mG, which, is still low compared with usual dose level.

The main source of systematic uncertainty in the thickness, SNR or contrast definitions (shown in Figs 11-13) for cases with and without reduction of scattering, is the uncertainty in the background definition. The background definition could be improved using a better signal description. So, it is necessary to use functions with more parameters for a better signal description as well as scatter reduction methods to improve the definitions of the above mentioned parameters.

4.1 SNR and Contrast

Contrast calculations have been done only to compare with other calculations and experimental data. The SNR and contrast in the simulated images for different μC thicknesses and for different beams are shown in Figs 12 and 13. No appreciable difference is observed between the SNR and contrast dependences on the μC thicknesses. The SNR dependence is more linear than the contrast and less sensitive to the scattered photon contribution. It is evident from Figs 12 and 13 that it is possible to improve SNR and contrast by approximately $\sim 17, 28\%$, respectively, using the “narrow” beam. This advantage is almost independent of the μC thickness up to the 1 mm region. Both parameters improve when the scanning beam size decreases. It seems possible to reach a $\sim 17\text{-}27\%$ improvement for the 3mm wide beam.

Results on contrast improvement using grid or scanning beam that we find in the literature are diverse. Differences in experimental data are large, going from no improvement at all [19] up to 50% [20, 4]. The M-C calculation in [2] predicts a 40% contrast improvement; the apparent discrepancy with these results can be explained from differences in geometry. In our case, one dimension of the scanning beam is limited to 2 cm and the contribution of scattered photons doesn’t reach its maximum possible value. As can be seen in Fig. 4, the background value depends on the distance of the beam to the phantom edge. Therefore, for the contrast defined by Eqn. (9) the improvement depends on the coordinate and will increase far away from

the boundaries.

In fact, image quality improvement can be explained using the statistical properties if the statistical noise is dominant. For a given incident exposure, for the low SNR values close to the detection threshold and with approximation signal \ll background, the SNR improvement parameter SI ($SI = SNR^{with}/SNR^{without}$, where SNR^{with} and $SNR^{without}$ are the signal to noise ratios with and without scatter reduction methods, respectively) can be written as:

$$SI = \frac{k_p \sqrt{1 + SPR}}{\sqrt{k_p + k_s SPR}} = k_p \sqrt{BF}, \quad (12)$$

where $k_p = N_p^{with}/N_p^{without}$, $k_s = N_s^{with}/N_s^{without}$, are the transmission coefficients for primary and scattered photons, respectively. N_p^{with} , $N_p^{without}$, N_s^{with} and $N_s^{without}$ are the numbers of primary and scattered photons with and without scatter reduction methods, respectively. BF is the Bucky factor of the scatter reduction grids[5, 21]. So, in case of using grids for scatter reduction and in order to have improvement in SNR without any additional dose, it is necessary to provide the following condition for the transmission coefficients:

$$k_p \geq \frac{1 + \sqrt{1 + 4k_s SPR(1 + SPR)}}{2(1 + SPR)}. \quad (13)$$

For scanning beams the primary photons transmission coefficients k_p are always 1 and the improvement depends on k_s and SPR . The SI maximum value only depends on the SPR value, and is equal to $SI_{max} = \sqrt{1 + SPR}$. To obtain a given value of $SI \leq SI_{max}$, the transmission coefficient of the scattered photons satisfies:

$$k_s = \frac{1}{SI^2} \left(1 - \frac{SI^2 - 1}{2SPR}\right) \quad (14)$$

For this transmission coefficient it is possible to calculate the beam sizes using the point spread function (see Fig 3).

4.2 Thickness

Results of the calculated μC thickness for the different beams are shown in Figs. 11 and 14. In Fig. 11 we show the thickness ratio for different dimensions of the scanning beams. For the "narrow" beam, the systematic uncertainty in the background definition is less than 1% (the flatness of the background for the "narrow" beam is $\sim 1\%$, see Fig 5). There is a $\sim 1\text{-}2\%$ systematic discrepancy between the calculated and the original thicknesses for the $200 \mu m$ calcification, which increases up to $3 - 4\%$ for the 1 mm thick μC . The $1 - 2\%$ disagreement could be related to differences in the mass attenuation coefficients used by GEANT during simulation and NIST data used for the thickness reconstruction. This source of systematic uncertainty is important only for the absolute thickness definitions and will be smaller for the thickness ratio definitions. Another possible source for this systematic uncertainty is the uncertainty in the calcium carbonate mass attenuation coefficient calculation.

The improvement of thickness determination when suppressing the scattering is approximately 35% for small thicknesses and increases up to 45 % for a 1 mm thick

calcification as shown by Fig 11. This improvement can be greater when using wider beams, since the contribution of scattered events can increase by 30% (see Fig. 3) and this would change the background by $\sim 10\%$. The dependence of the thickness improvement on the beam size in the scanned direction for the different μC thickness is shown in Fig 14. The improvement for all μC thicknesses will decrease with beam size and for the 3mm wide beam it will reach of 85-95 % of the "narrow" beam.

We have not been able to find published experimental information about the use of the thickness determination. There are data for visual contrast improvement[4]. This concept is equivalent to thickness improvement, since the attenuation coefficients cancel out in ratio. Data for VC [4] for phantom sizes $12.4 \times 12.4 \times 4 \text{ cm}^3$ (50/50% adipose /glandular) phantom with different exposed beams and grid types show maximal VC improvement, up to 50% (uncertainty $\sim 5\%$). Our results agree with these data, taking into account geometrical and phantom differences.

4.2.1 μC position uncertainty Everything mentioned above is correct when the μC target positions are known. Usually, the μC positions in the breast are unknown and calculations of the absorption coefficient averages (see 4) are problematic, among other reasons, because photon spectrum will strongly depend on the depth of the point in the phantom. In our case, the μC absorption coefficient mean values have been calculated assuming the photon spectrum at the center of the phantom. The systematic uncertainty introduced by this simplification may be estimated for the 25 kVp Mo/Mo spectrum and 4 cm thick phantom assumed in this study, as being $\sim 2.5\%$ in D_μ . This value could be decreased, at least twice, using additional filters that narrow the energy spectrum. These systematic uncertainties will increase with total phantom thickness. To make microcalcification thickness measurements independent of the breast thicknesses it would be necessary to use mono-energetic photon beams.

Conclusion

We have preformed Monte-Carlo simulation of 25 kVp Mo/Mo X-rays transported in a 4 cm thick breast phantom. We have focused on the reconstruction of the thicknesses of 0.2-1.0 mm thick microcalcifications embedded in the phantom. We have shown the possible thickness reconstruction with an accuracy of the order of 6% using a 3 mm wide slot scanning beam. This slot size, which seems to be technically feasible, for a mammography unit promises results which are close to the ideal narrow beam. The same beam could improve the signal-to-noise ratio by $\sim 20\%$, similar to the effect of using ideal narrow beam.

The μC thicknesses parameter can be used as alternative to SNR for microcalcification detection. The use of semi mono-energetic photon beams would decrease systematic uncertainties in μC thicknesses determination. One of the goals of this calculation was to show that the GEANT code is appropriate for digital mammography calculations.

Acknowledgments

Authors thank partial support from DGAPA-UNAM, Grant IN-109302

References

- [1] Barnes G.T. and Brezovich I.A. 1978, The intensity of scattered radiation in mammography, *Radiology* **126** (1) 243.
- [2] Boone J.M. and Cooper V.N. III 2000, *Med Phys.* **27** (8) 1818
- [3] Barnes G.T. 1994 Technical Aspects of Breast Imaging *Radiological Society of North America* 74 Oak Brook, IL.
- [4] Rezentes P.S., Almeida A. De and Barnes G.T. 1999, Mammography grid performance, *Radiology* **210** 227.
- [5] Barnes G.T., Wu X. and Wagner A.J. 1993, Scanning slit mammography *Medical Progress through Technology* **19** 7.
- [6] Yester M.V., Barnes G.T. and King M.A. 1981 Experimental measurements of the scatter reduction obtained in mammography with a scanning multiple slit assembly *Med. Phys.* **8** (2) 158.
- [7] Neitzel U. 1992 Grids or air gaps for scatter reduction in digital radiography: A model calculation *Med. Phys.* **19** (2) 475.
- [8] Dowsett D. J., Kenny P.A. and Johnston R.E. 1998, The Physics of diagnostic imaging *Chapman & Hall Medical* London.
- [9] L. Steven *et al* 1983 *Med Phys.* **10** (6) 866.
- [10] NIST DATA <http://physics.nist.gov/PhysRefData/XrayMassCoef/cover.html>
- [11] Lemacks M.R. *et al* 2002 *Med Phys.* **29** (8) 1739
- [12] Users Guides: <http://geant4.web.cern.ch/geant34/G4UsersDocuments>
- [13] Attix F.H. 1986 Introduction to radiological physics and radiation dosimetry *A Wiley-Interscience Publication* New York.
- [14] Paganetti H. and Gottschalk B. 2003 *Med Phys.* **30** (7) 1926.
- [15] Fewell T.R. and Shuping R.E. 1978 Handbook of Mammographic X-Ray Spectra, *Rockville, BRH (FDA)*.
- [16] Boone J.M. 1999 *Radiology* **213** 23.
- [17] ROOT: <http://root.cern.ch/root/RootDoc.html>
- [18] Boone J.M. 2000 *et al* *Med Phys.* **27** (10) 2408.
- [19] Veldkamp W.J.H. , Thijssen M.A.O. and Karssemeijer N. 2003 *Med Phys.* **30** (7) 1712.
- [20] Boone J.M. *et al* 2002 *Radiology* **222** 519.
- [21] Fahrig R. *et al* 1994 *Med Phys.* **21** (8) 1277.

Table 1. Chemical composition by weight, of the phantom materials. Values are taken from NIST[10]

Z	Adipose tissue	Glandular tissue	Microcalcification($CaCO_3$)
1	0.114	0.106	-
6	0.598	0.332	0.12
7	0.007	0.03	-
8	0.278	0.527	0.48
11	0.001	0.001	-
15	-	0.001	
16	0.001	0.002	
17	0.001	0.001	
20	-	-	0.40

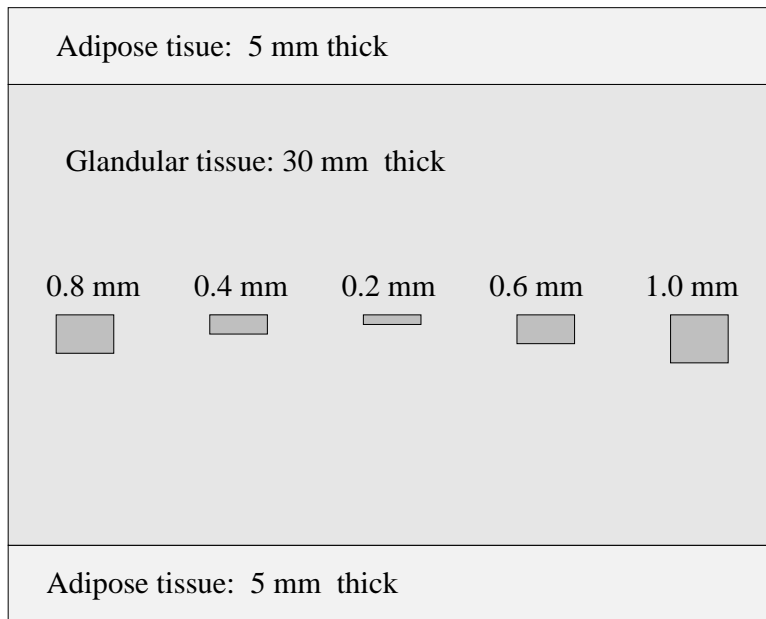


Figure 1. Phantom structure. Calcification thickness is indicated. Cylindrical microcalcifications are 4 mm in diameter.

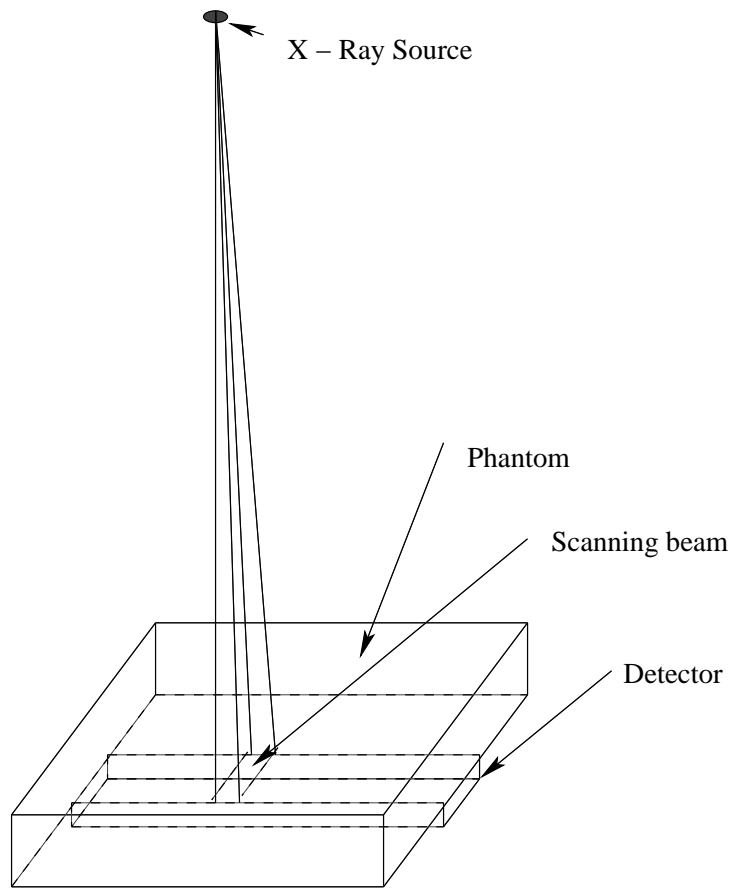


Figure 2. Simulation setup

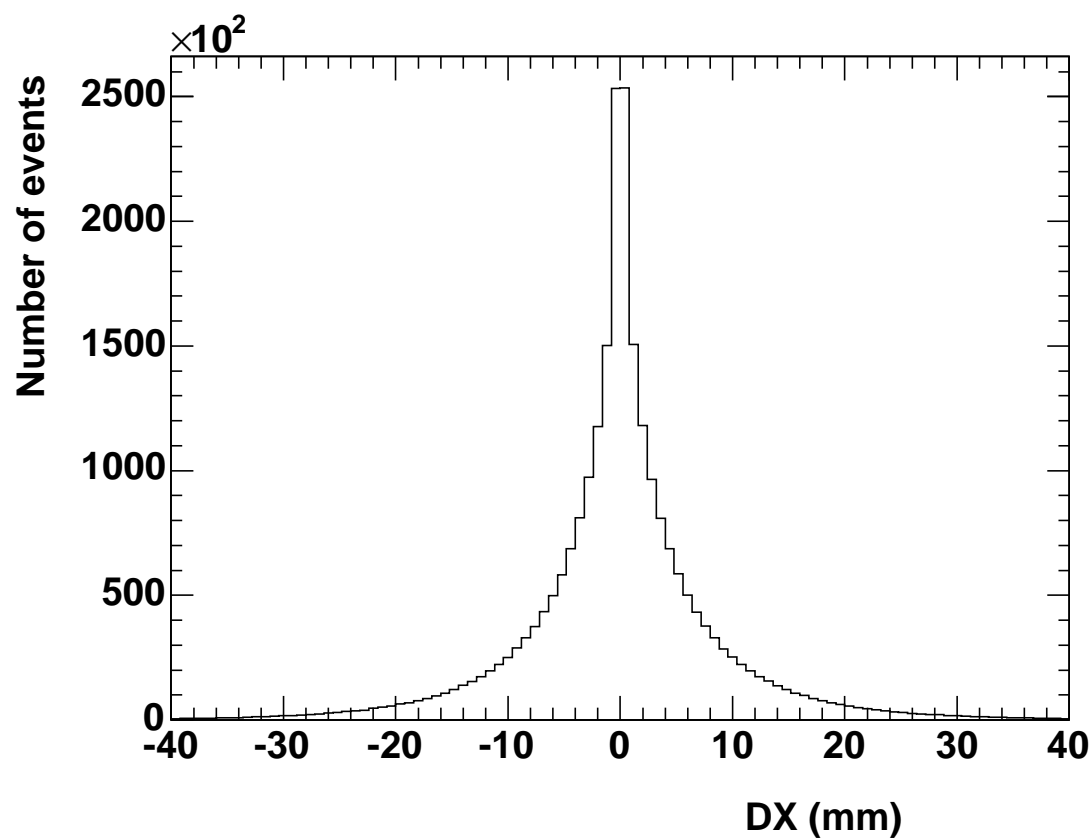


Figure 3. Point spread function for scattered photons (see text)

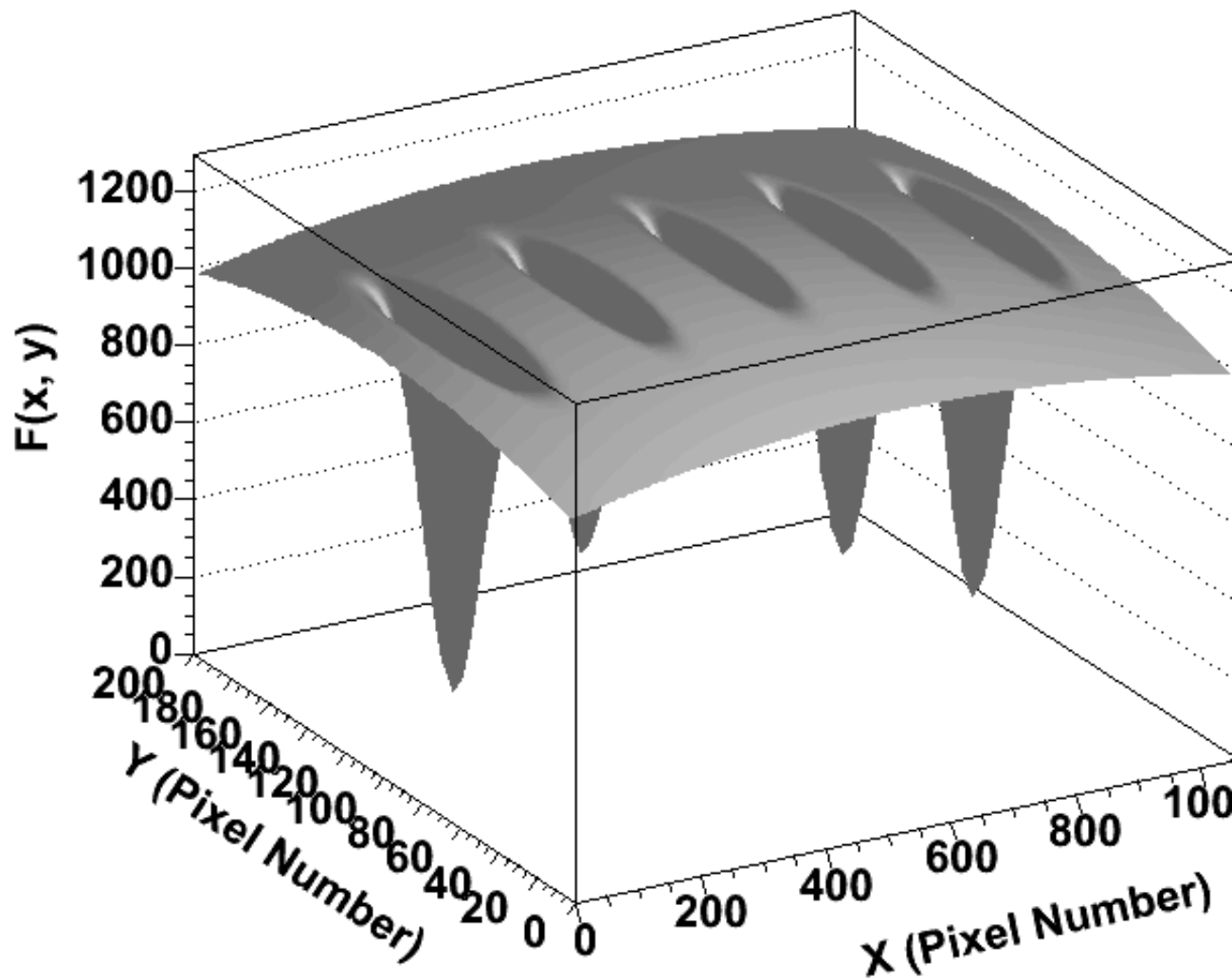


Figure 4. Signal and background description by a multi-parameter function $F(x, y)$ in the case NSR, without scanning (see text)

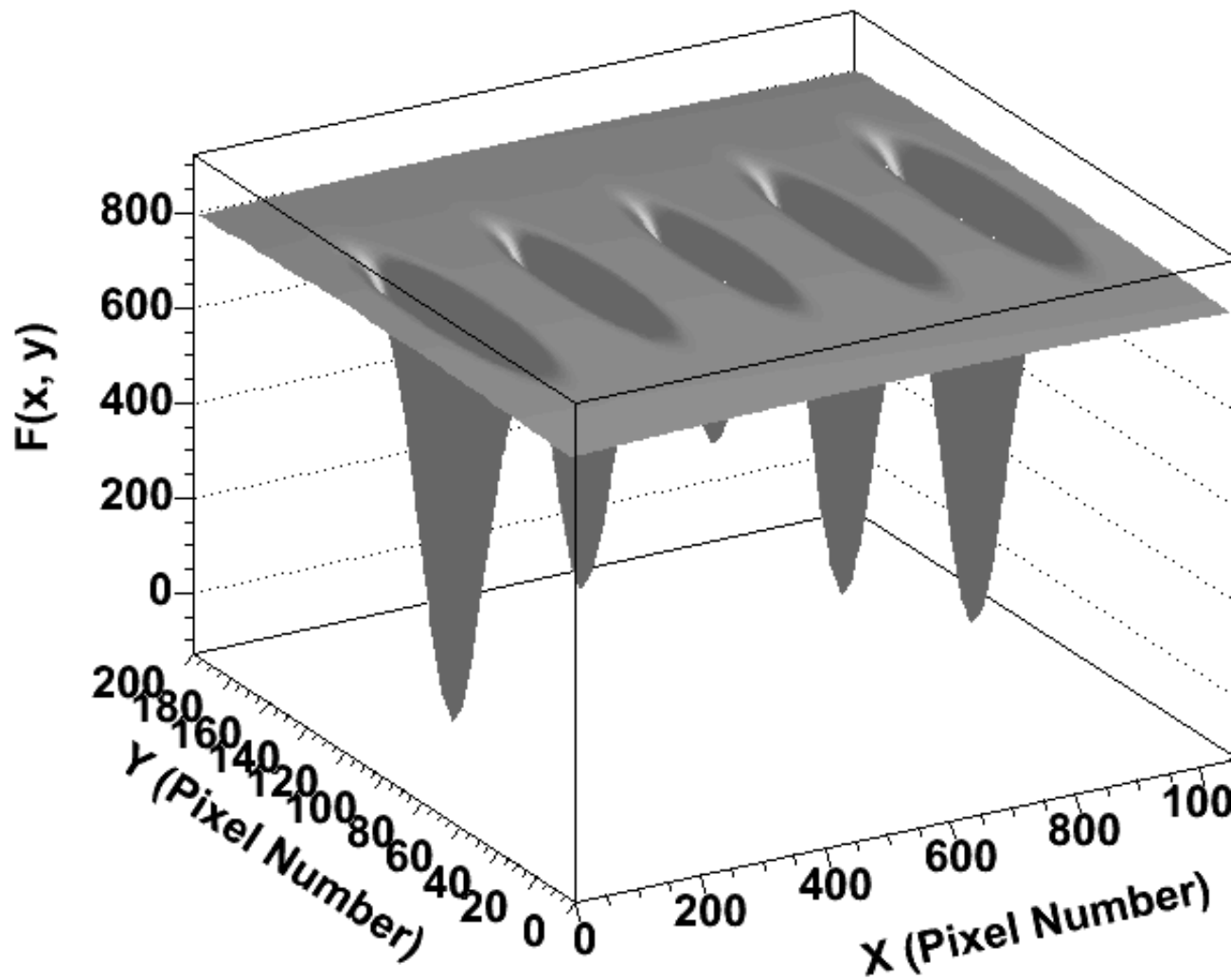


Figure 5. The same as in Fig 4 for case of the “narrow” beam (see text)

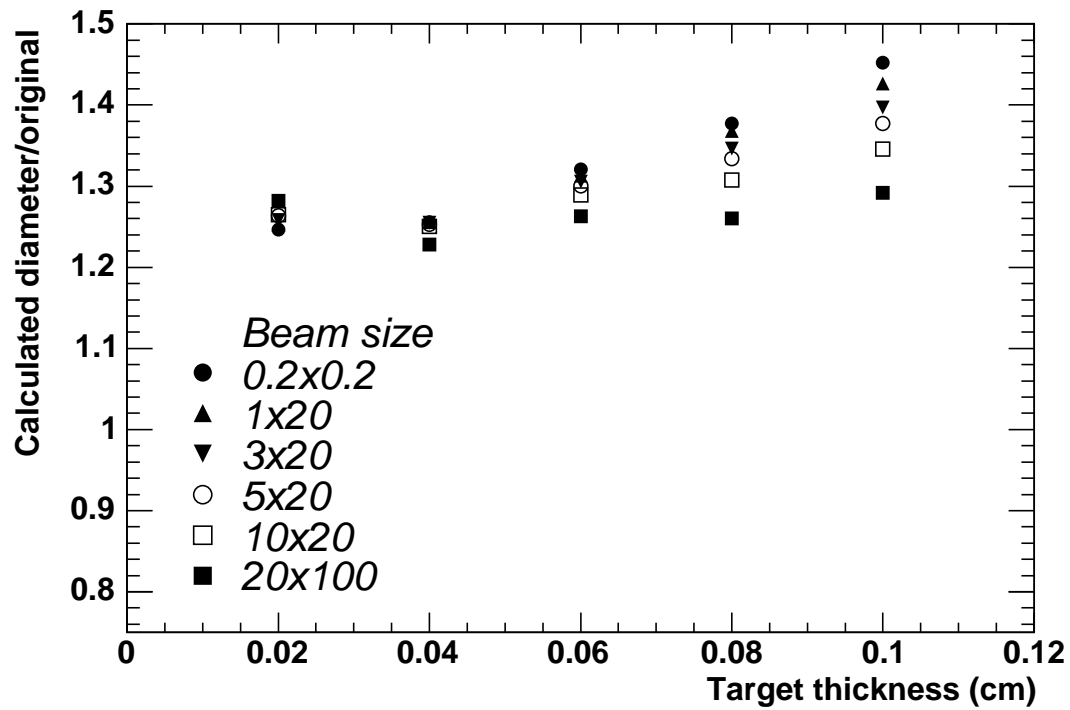


Figure 6. Calculated μC diameter ($\sigma_{\mu C}^{fit} \sqrt{3}$) as a function of the microcalcification thickness. Beam sizes are in mm^2 .

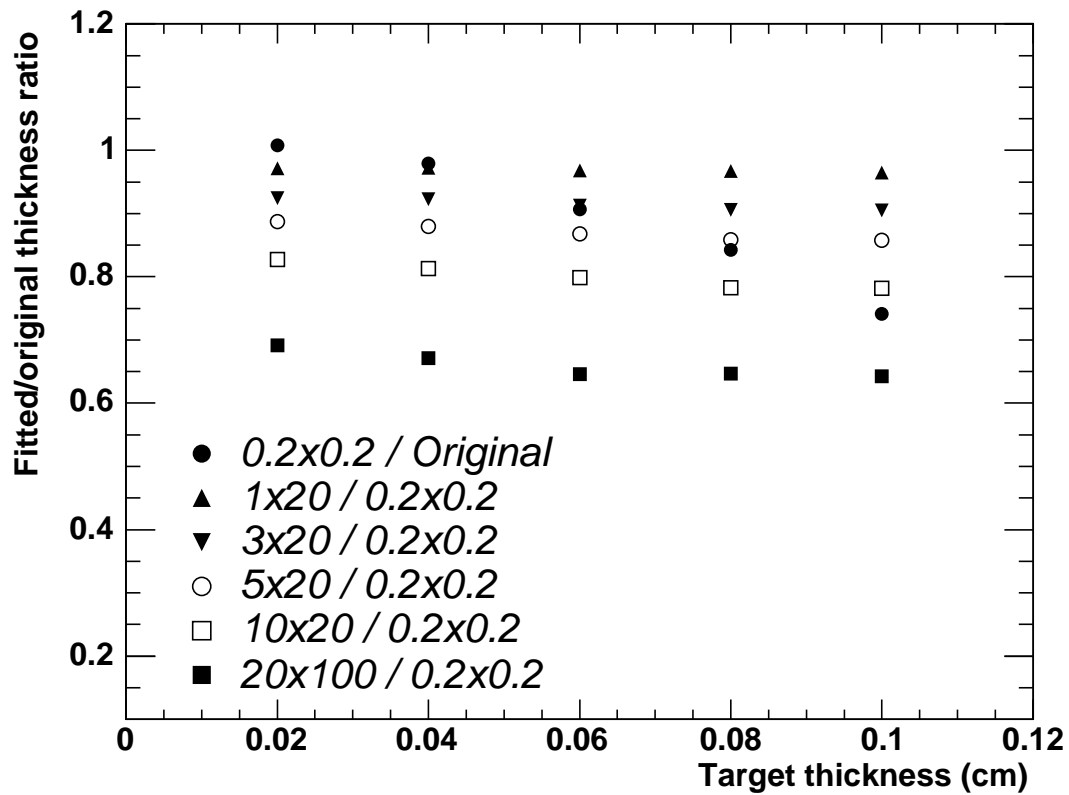


Figure 7. Thickness calculation (t_f) using the function $F(x, y)$ (see text). Beam sizes are in mm^2 .

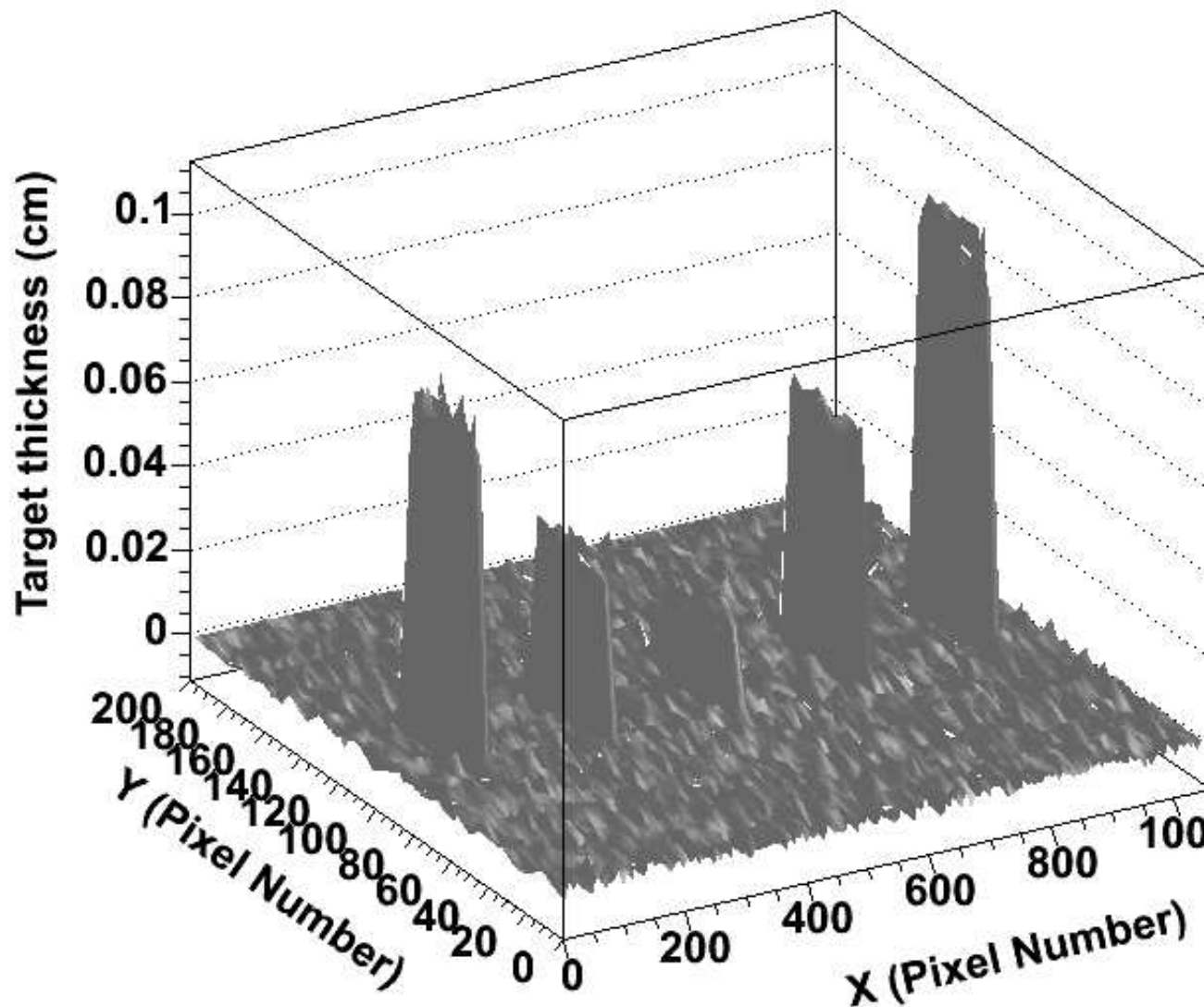


Figure 8. Reconstructed 3D-image of the thicknesses for the “narrow” beam. Original thicknesses are 0.08, 0.04, 0.02, 0.06 and 0.1 cm, from left to right.

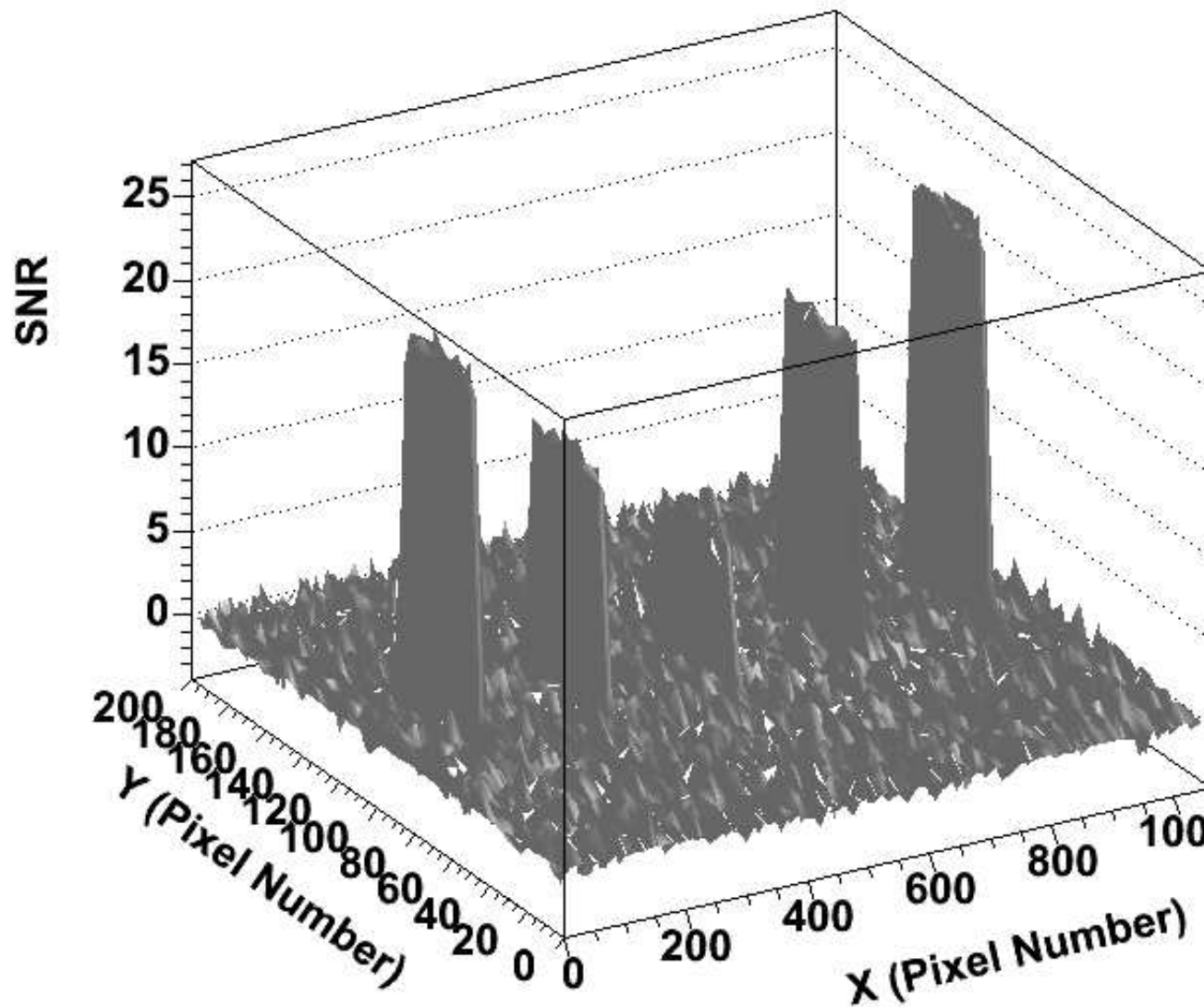


Figure 9. Reconstructed 3D-image of the *SNR* for the “narrow” beam.

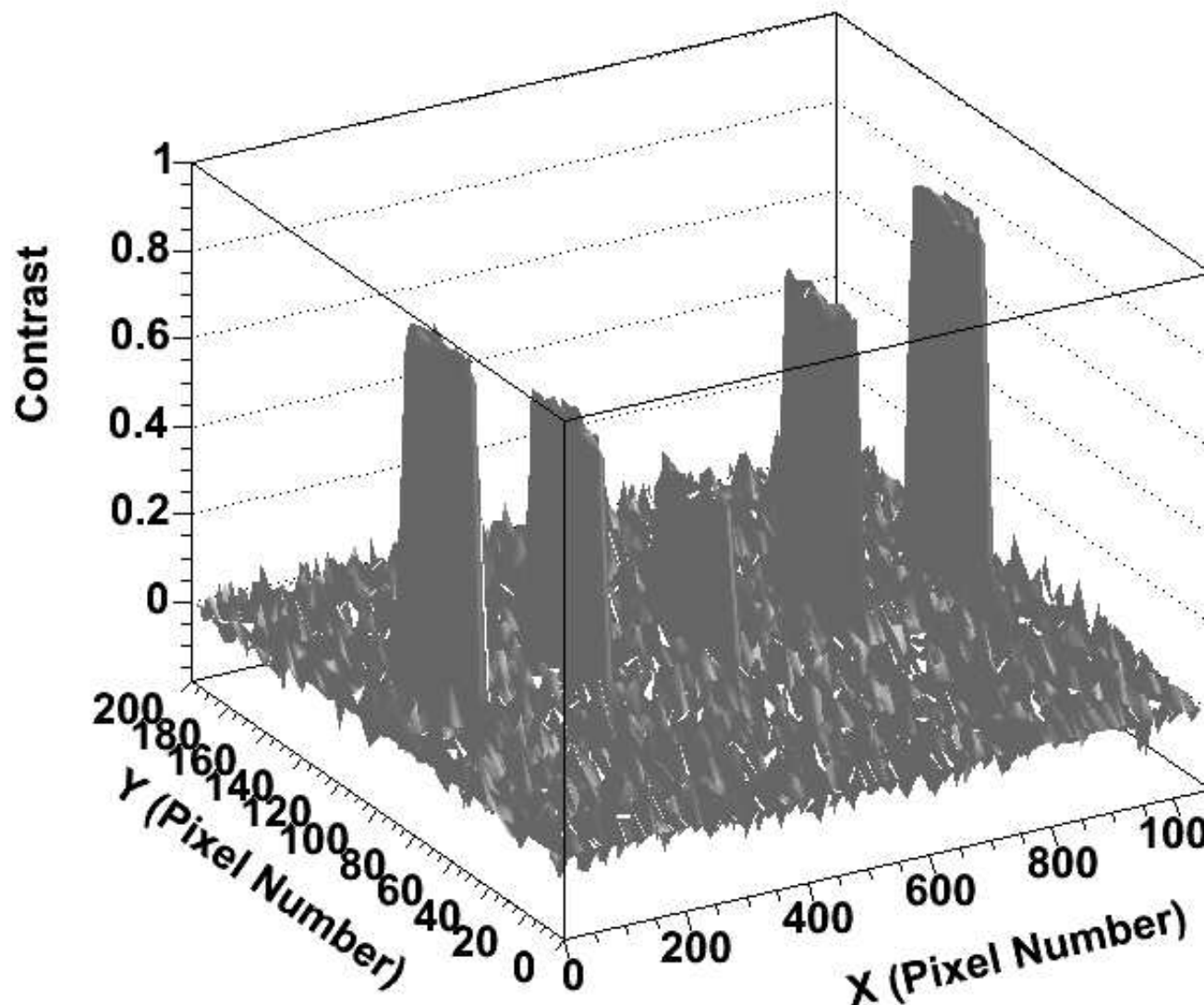


Figure 10. Reconstructed 3D-image of the contrast for the "narrow" beam .

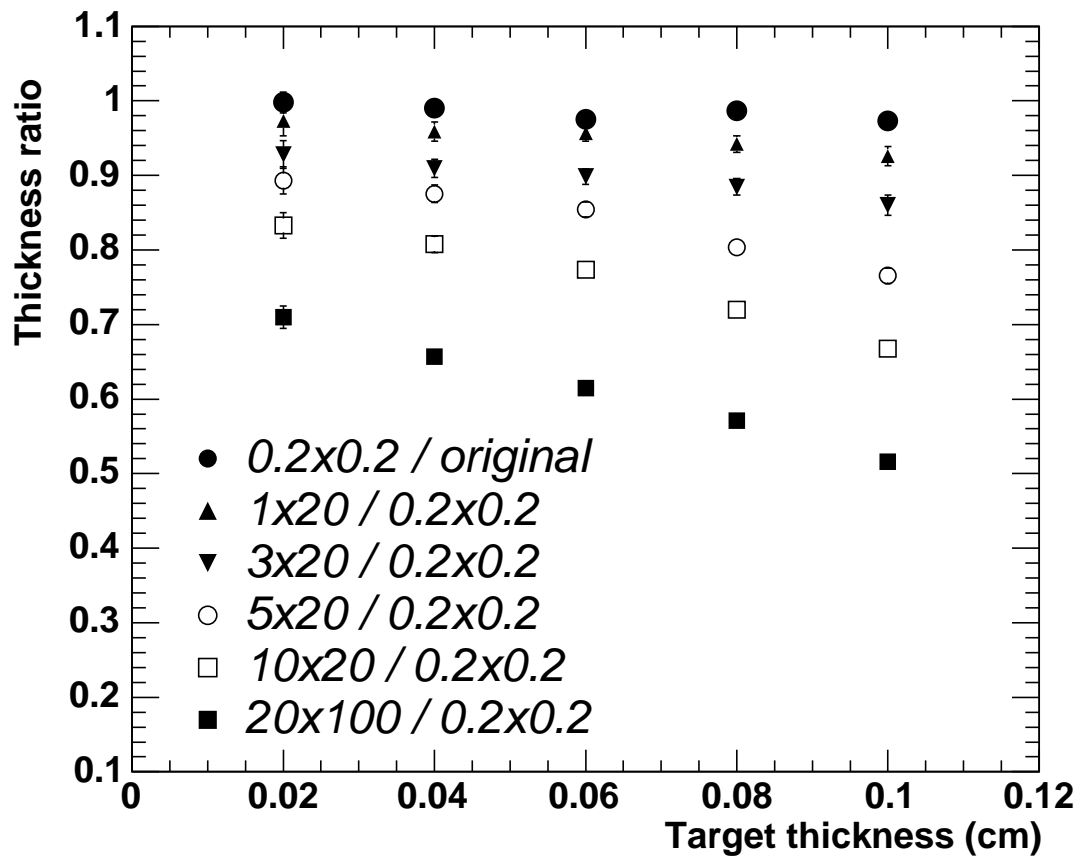


Figure 11. The thickness ratio (with respect to the original thickness for the narrow beam, and ratios for the rest) in the simulated images using the polynomial background definition, and its dependence on the μC thicknesses for the different beams. Beam sizes are in mm^2

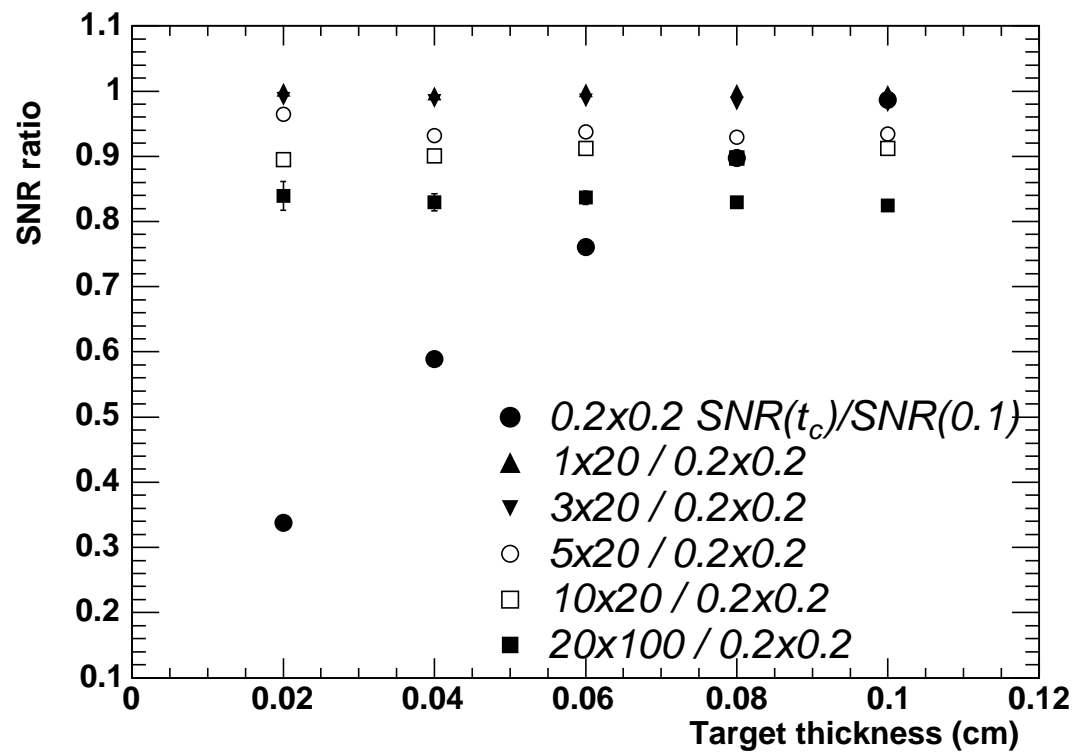


Figure 12. The SNR ratio in the simulated images using the polynomial background definition, and its dependence on the μC thicknesses for the different beams. Beam sizes are in mm^2 .

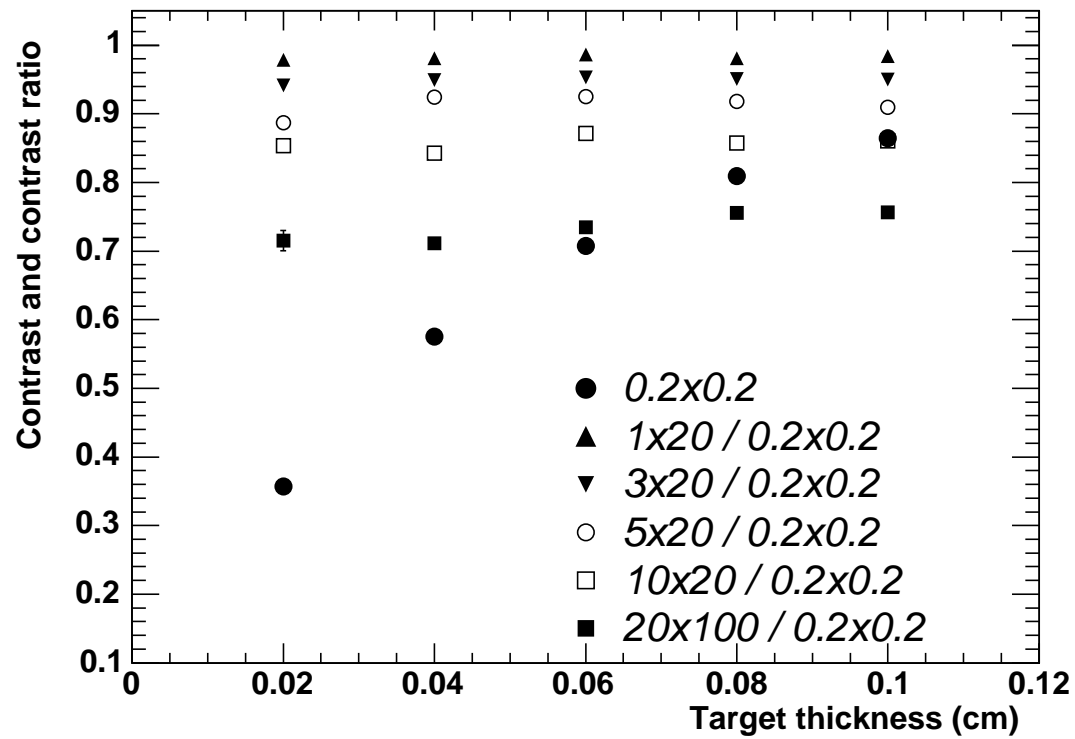


Figure 13. The contrast (value for the “narrow” beam and ratio value for the rest) in the simulated images using the polynomial background definition, and its dependence on the μC thicknesses for the different beams. Beam sizes are in mm^2 .

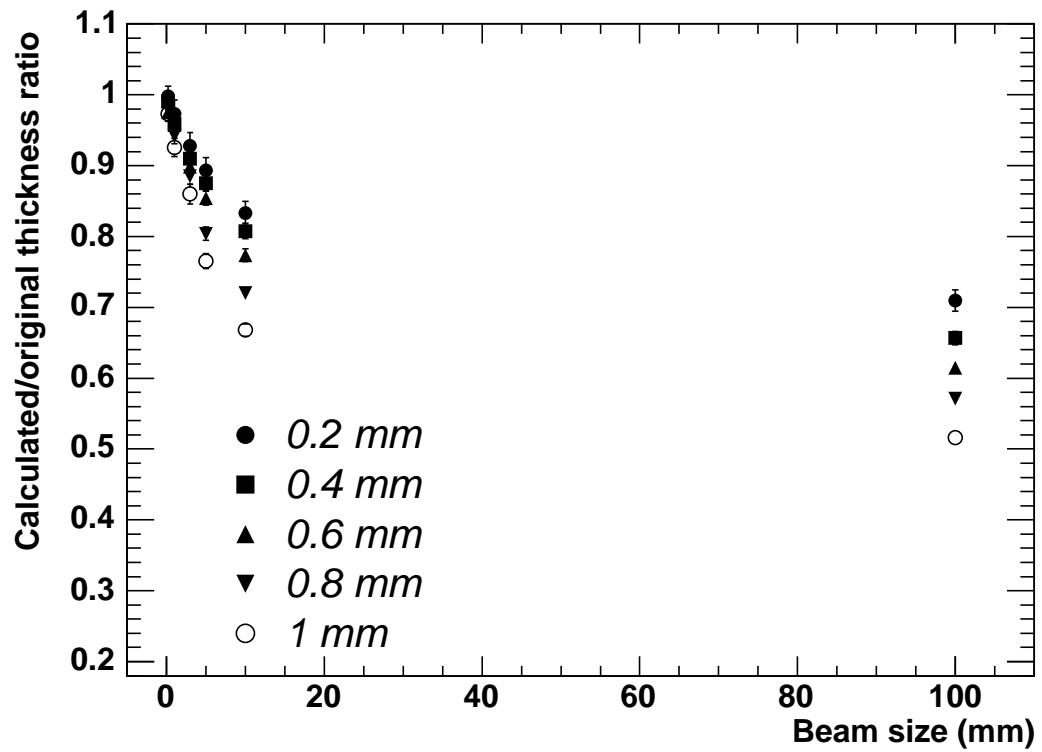


Figure 14. Dependence of the thickness ratio (calculated/original) on the beam size along the scanning direction (see Fig. 2). Different symbols correspondent the original calcification thickness.